

























































































































































































































































# Solar assisted absorption cooling cycles for reduction of global warming: a multi-objective optimization approach

Berhane H. Gebreslassie<sup>a</sup>, Gonzalo Guillén-Gosálbez<sup>b</sup>, Laureano Jiménez<sup>b</sup>,  
Dieter Boer<sup>a,\*</sup>

<sup>a</sup>*Departament d'Enginyeria Mecànica, Universitat Rovira i Virgili  
Av. Països Catalans, 26, 43007, Tarragona, Spain*

<sup>b</sup>*Departament d'Enginyeria Química, Universitat Rovira i Virgili  
Av. Països Catalans, 26, 43007, Tarragona, Spain*

---

## Abstract

This work studies the use of absorption cycles combined with solar energy for reducing the green house gas emissions in the energy sector. The problem of satisfying a given cooling demand at minimum cost and environmental impact is formulated as a bi-criterion nonlinear optimization problem that seeks to minimize the total cost of the cooling application and its contribution to global warming. The latter metric, which is assessed following the principles of life cycle assessment, accounts for the impact caused during the construction and operation of the system. The concept of Pareto optimality is employed to discuss different alternatives for reducing the contribution to global warming that differ in their economic and environmental performance. We show that reducing the contribution to global warming considering the current energy prices and taxes on carbon dioxide emissions is technically viable but economically not appealing. We also discuss the conditions under which reducing the  $CO_2$  emissions could become economically attractive.

*Keywords:* Solar assisted cooling, NLP, Multi-objective optimization, Life

---

\*Corresponding author

*Email address:* Dieter.Boer@urv.cat (Dieter Boer )



cycle assessment (LCA), Global warming potential

---

## 1. Introduction

The human pattern of development has led to a significant increase in greenhouse gas (GHG) emissions and consequently in global warming [1]. Based on the Intergovernmental Panel on Climate Change (*IPCC*) [2] global GHG emissions increased by 70% between 1970 and 2004, growing from 28.7 to 49 Gigatonnes of carbon dioxide equivalents ( $GtCO_{2eq}$ ).  $CO_2$  emissions grew by 80% in the same period representing 77% of the GHG emissions in 2004.

Nowadays, 94% of the  $CO_2$  emissions in Europe are attributed to the energy sector as a whole, and particularly to the combustion of fossil fuels. Oil consumption accounts for 50% of the  $CO_2$  emissions in the European Union, natural gas for 22% and coal for 28% [1]. Particularly, the building sector represents 40% of the total primary energy demand in European Union countries and it is responsible for one third of the GHG emissions [3].

A large percentage of the emissions attributed to the building sector are due to air conditioning (AC) systems, most of which are based on electricity driven compression cycles. These systems show the best economic performance and for this reason they have dominated the market in the last years. Unfortunately, they consume non-renewable primary energy resources and contribute to major environmental problems such as the Ozone layer depletion (due to the refrigerants) and global warming (because of their electricity consumption [4]). With the recent trend of developing more sustainable processes, there has been a growing interest on thermal energy activated cooling machines. These systems represent an environmentally friendly alternative to standard compression chillers, as they can be driven by waste heat, natural gas, solar energy or biomass. This can lead to significant reductions in GHG emissions [5–7].

Among all the alternatives to standard AC systems, solar assisted cooling cycles are seen by many as a promising option. By using solar energy

autonomous cooling systems, it is possible to achieve virtually zero  $CO_2$  emissions. Unfortunately, the current electricity cost and fuel prices make it difficult to compete with conventional cooling systems [8]. Hence, the adoption of alternative AC systems raises the question of to which extent decision-makers are willing to compromise the economic performance in order to obtain environmental benefits.

Mathematical programming methods, and in particular, multi-objective optimization, offer a suitable framework for addressing this type of problems. These techniques allow for the inclusion of environmental concerns in the decision-making process by generating a set of trade-off solutions that balance economic and environmental criteria called the Pareto set. From these points, decision-makers can identify the best ones according to their strategic guidelines and applicable legislation.

Several optimization studies have been carried out on cooling systems [13–16]. Most of them addressed the optimization of the economic performance of the cooling application and neglected the associated environmental impact. A reduced number of approaches have applied multi-objective optimization to the design of energy systems [17–19]. However, to our knowledge, none of them focused on integrated solar absorption systems.

One of the key issues in multi-objective optimization as applied to environmentally conscious process design is the definition of a suitable environmental metric. Works incorporating environmental concerns through multi-objective optimization have typically focused on minimizing the impact at the plant level [19, 20], thus neglecting the damage caused in other stages of the life cycle. This approach can lead to solutions that transfer the environmental problem to other echelons of the energy supply chain, thereby failing in reducing the environmental damage globally [21]. A proper evaluation of the environmental performance of a system requires the application of life cycle assessment (LCA) principles [11, 12, 22, 23] for quantifying the impact from the extraction of raw materials to the delivery of energy to the final customer. Despite recent advances in LCA methodology, the current

situation is that the literature on the application of LCA to energy systems is limited.

With the aforementioned observations in mind, the goals of this work are: (i) to perform an LCA analysis on solar assisted absorption cooling systems; and (ii) to explore their environmental benefits in terms of reducing the GHG emissions by employing a multi-objective optimization framework. Specifically, in this work we will elaborate, among others, the following points.

- i. Under which circumstances the use of solar energy in cooling applications is economically competitive with fossil fuels? (*i.e.*, which are the values of the fuel cost and  $CO_2$  taxes that make the use of solar energy in absorption cooling systems profitable?)
- ii. How much can be saved in terms of GHG emissions by integrating solar collectors with absorption cooling systems?

This work is structured in seven sections. The section that follows presents a motivating example that illustrates the environmental benefits of the solar assisted absorption chiller over the counter part vapor compression cycle. The next section discusses the mathematical formulation of the multi-objective optimization problem. Special emphasis is given to the solar system performance constraints and the equations added to quantify the environmental impact (*i.e.*, contribution to global warming). The fourth and fifth sections concentrate on the solution method of the problem and the case study used to test its capabilities. A detailed discussion of the results is presented in section six. The conclusions of the work are finally drawn in the last section of the paper.

## 2. Motivating example

We present first a straightforward example that helps to briefly illustrate the environmental advantages of integrating solar collectors with absorption cycles for reducing the GHG emissions in cooling applications. Three chillers,

the conventional electricity driven one and two thermal energy driven chillers, are considered at this point. Particularly, we will study single effect absorption and vapour compression cycles with coefficients of performance of 0.7 and 3, respectively. The vapour compression cycle motor efficiency ( $\eta^{mot}$ ) is 95%. The solar fraction ( $SF$ ) of the absorption chillers are 0% (100% natural gas) and 70%. A life span of 20 years and 2000 working hours per year are assumed.

These systems are compared in terms of their global warming potential (GWP) expressed in equivalent tons of  $CO_2$  per unit of cooling capacity generated. In the case of the electricity driven chiller, the calculation of the GWP accounts only for the electricity generation. For the thermal energy driven chillers, the environmental analysis considers the extraction and combustion of natural gas as well as operation of the solar collectors. It should be noted that, for the sake of simplicity, in both cases the impact associated with the construction of the cycle has been neglected. The electricity consumed by the pump of the absorption cycle has also been neglected, since it represents a very low percentage of the total energy consumption. With regard to the GWP associated with the electricity generation, we consider different electricity generation mixes (*i.e.*, Spain, USA and China). The associated GWP values per unit of energy generated have been retrieved from the environmental database Ecoinvent [24]. For the countries considered in this example, these are 0.6035, 0.751 and 1.148 [ $kg CO_{2eq}/kWh$ ], respectively. On the other hand, the GWP due to the combustion of natural gas in the gas fired heater, which has also been retrieved from Ecoinvent, is 0.256 [ $kg CO_{2eq}/kWh$ ]. The latter value includes also the impact associated with the construction of the boiler.

**[Figure 1 Could be placed here]**

The results of the analysis are shown in Fig. 1. Particularly, Fig. 1(a) represents 100 kW cooling capacity powered by natural gas. The total GWP

is 1463  $ton CO_{2eq}$  with a natural gas consumption of 142.8 kW. Fig. 1(b) represents the same cycle but this time powered by combination of natural gas and solar energy. With this integration, the natural gas consumption drops to 42.9 kW, with a total GWP of 438.8  $ton CO_{2eq}$ . Fig. 1(c) represents a 100 kW cooling capacity vapour compression cycle powered by electricity. The GWP of this chiller is 847, 1054 and 1612  $ton CO_{2eq}$  in Spain, USA and China, respectively.

Comparing chillers (a) and (b), it can be seen that it is possible to reduce up to 70% the primary energy demand of the cycle by integrating it with solar energy. This reduces the GWP from 1463 to 438.8  $ton CO_{2eq}$ .

The comparison between chillers (a) and (c) depends on the electricity production mix. The use of absorption chillers in China reduces the GWP by 9%. On the other hand, in Spain and USA, vapour compression chillers are environmentally more attractive than the considered absorption chillers. It should be noted that absorption chillers become competitive from an environmental perspective if they had higher COPs. This could be accomplished by using double or triple effect configurations. Besides, their impact could also be reduced by using less contaminant heat sources or free driving energy as waste heat.

The comparison between chillers (b) and (c) reveals that solar assisted absorption chillers are environmentally more attractive than electric chillers. The magnitude of the GWP reduction depends again on the electricity production mix of the country. We can see from the results that reductions in GWP of 48%, 52% and 73% can be achieved in Spain, USA and China, respectively. In these cases, the advantages are twofold: (i) the mitigation of global warming; and (ii) the reduction in the consumption of those non-renewable primary energy resources consumed for generating the electricity required by the compression chillers.

### **3. Mathematical formulation: a multi-objective optimization approach**

After proving the environmental advantages of integrating solar collectors with absorption cycles, we next derive a multi-objective mathematical formulation for analyzing systematically these systems considering environmental and economic criteria simultaneously.

#### *3.1. System description*

In order to derive our formulation, we consider a typical ammonia/water mixture supported solar assisted absorption chiller (see Fig. 2). The detail description of the absorption cycle could be found [14]. It is assumed that the heat demand required to activate the chiller can be supplied either by the gas fired heater using natural gas as primary energy resource or by solar energy captured by solar collectors. Evacuated tube collectors are used to convert the solar energy into usable forms of thermal energy. It is also possible to cover the heat demand of the absorption chiller by a combination of the aforementioned heat sources.

**[Figure 2 could be placed here]**

The problem addressed in this paper can be formally stated as follows. Given are the cooling capacity of the cooling system, the inlet and outlet temperatures of the external fluids (except the generator temperatures), capital cost data, monthly weather data (ambient temperature and global daily solar radiation), performance equations of the solar collector, and GHG emissions associated with the construction and operation of the cooling system. The goal is to minimize simultaneously the contribution to global warming and the total cost of the cooling system.

#### *3.2. Mathematical formulation*

We present next a multi-objective optimization model that provides as output a set of technical alternatives for satisfying the cooling demand, each

featured by a different economic and environmental performance. The mathematical model of the absorption cycle is based on the formulation presented in detail in previous works [14, 25]. The model described here extends the original formulation by integrating the absorption cycle with solar collectors. For completeness of the work, we present the main equations of the absorption cycle already described elsewhere [14, 25] in the Appendix. On the other hand, the solar collector performance constraints and the equations associated with the calculation of the GHG emissions are given next.

The mathematical formulation is a multi-period one that allows to follow a given cooling demand pattern while accounting for varying meteorological conditions over time. It is assumed that the cycle can operate in a different manner in each time period  $t$  in order to get adapted to the specific solar radiation available. The model is based on mass and energy balances (see Appendix) and objective function constraints that allow to assess the economic and environmental performance of the cooling system.

### 3.2.1. Heat production subsystem

The model considers that the heat supplied to the absorption cycle is provided from the solar collectors and the gas fired heater. The associated solar collector constraints are presented in the following sections.

### 3.2.2. Collector performance constraints

Solar collectors absorb solar radiation and convert it into useful heat. The useful heat collected is transported by working fluids flowing through the solar collectors [26]. The collector performance is denoted by a continuous variable  $\eta_t^{col}$  whose value is determined via eqn. (1). On the other hand, the heat collected from the solar collector in period  $t$  ( $Q_{k=col,t}$ ) is given by eqn. (2).

$$\eta_t^{col} = IAM(\Theta)c_0 - c_1 \frac{T_t^{av} - T_t^{amb}}{G_t} - c_2 \frac{(T_t^{av} - T_t^{amb})^2}{G_t} \quad \forall t \quad (1)$$

$$Q_{k,t} = \eta_t^{col} A_{col} G_t \quad k = Col, \forall t \quad (2)$$

In eqn. (1),  $IAM(\Theta)$  is the incident angle modifier, which accounts for the effect of a non perpendicular incident radiation at incidence angle  $\Theta$  in relation to a normal incidence radiation (*i.e.*,  $\Theta = 0$ );  $T_t^{av}$  is the monthly average inlet and exit fluid temperature in the collector; and  $T_t^{amb}$  is the monthly average ambient air temperature. The daily global solar radiation is represented by  $G_t$ . Finally,  $c_0$  denotes the optical efficiency of the collector, whereas  $c_1$  and  $c_2$  are the linear and quadratic loss coefficients, respectively [8]. On the other hand, in eqn. (2),  $n$  represents the number of collectors and  $A_{col}$  is the absorber area of a single collector. For the sake of simplicity, in this work we treat the integer variable  $n$  as a continuous one. It should be noted that from numerical examples we have observed that this can be done without compromising the quality of the final solution. This simplification greatly helps the computations.

### 3.2.3. Linking constraints

Eqn. (3) relates the heat consumed by the absorption cycle with that produced by the solar collector and the gas fired heater. More precisely, the sum of the heat produced by the solar collector ( $Q_{k=Col,t}$ ) and gas fired heater ( $Q_{k=GFH,t}$ ) should cover at least the heat demand ( $Q_{h=D,t}$ ) of the absorption cycle in period  $t$ .

$$Q_{k,t} \leq Q_{k',t} + Q_{k'',t} \quad k = D, k' = Col, k'' = GFH, \forall t \quad (3)$$

Furthermore, the heat produced by the heater in every time period must be less than or equal to its capacity ( $CAP_{k=GFH}$ ) as given by eqn. (4).

$$Q_{k,t} \leq CAP_k \quad k = GFH, \forall t \quad (4)$$

### 3.3. Objective functions

The model seeks to minimize two contradicting objective functions simultaneously: total cost and contribution to global warming. Details on the calculations of both performance metrics are given in the next subsections.



### 3.3.1. Economic performance

The economic assessment of the absorption cycle is discussed in detail in [14, 25]. Specifically, the total cost (TC) accounts for the capital and operating cost of the integrated system ( $TCC$  and  $TOC$ , respectively) as shown in eqn. (5).

$$TC = TCC + TOC \quad (5)$$

In this equation,  $TCC$  accounts for the cost of the heat exchangers of the cycle, solar collectors, gas fired heater, pump and expansion valves. On the other hand, the operating cost ( $TOC$ ) includes the running cost of the gas fired heater, pump and solar collectors, as well as the cooling water cost. The capital and operation cost constraints are included in the Appendix.

### 3.3.2. Environmental impact

The environmental impact is quantified according to LCA principles. The combined use of LCA and multi-objective optimization has been shown to be a suitable framework for identifying, in a systematic way, opportunities for environmental improvements in different applications [9–12]. In this approach, LCA is employed to assess the environmental performance of a system, whereas optimization techniques enable us to generate feasible process alternatives and identify the best ones in terms of economic and environmental criteria. General details on the LCA methodology can be found elsewhere [21].

The calculation of the life cycle impact of the cooling application follows the four LCA steps: (1) goal and scope definition; (2) inventory analysis; (3) damage assessment; and (4) interpretation. We describe next these phases in the context of our study.

*Goal and scope definition:* In this step, the system boundaries, the functional unit and the environmental damages are defined. We perform a cradle-to-gate analysis that accounts for the generation of the utilities consumed by the cooling system as well as the impact during the construction phase. The functional unit is the amount of cooling demand satisfied during the time

horizon. The environmental damage is quantified through the global warming potential (GWP). This is a measure of how much a given mass of a GHG emission contribute to global warming. It is a relative scale which compares the impact of a given chemical with that of the same mass of carbon dioxide (whose GWP by convention equals 1). The GWP is calculated over a specific time interval that must be stated beforehand [2, 27]. Particularly, we follow the Intergovernmental Panel on Climate Change IPCC 2007 framework considering a time horizon of 100 years, which is the time frame used in the Kyoto Protocol [27].

*Inventory analysis:* This step aims at quantifying the total GHG emissions associated with the absorption cooling. These emissions are represented by a continuous variable ( $LCI_b^{tot}$ ), that is determined from the emissions during the manufacturing ( $LCI_b^{man}$ ) and operation ( $LCI_b^{op}$ ) of the cooling system, as shown in eqn. (6).

$$LCI_b^{tot} = LCI_b^{man} + LCI_b^{op} \quad \forall b \quad (6)$$

The life cycle GHG emissions during the construction phase, which are denoted by the continuous variable  $LCI_b^{man}$ , can be determined from the sizes of the gas fired heater, solar collectors, heat exchangers and pumps of the cycle, as stated in eqn. (7).

$$LCI_b^{man} = \sum_k LCIE_{b,k} CAP_k \quad (7)$$

Here, the continuous variable  $CAP_k$  represents, in each case, the mass of the heat exchangers and expansion valve in  $kg$ , heat capacity of the gas fired heater and pump capacity expressed in  $kW$ , power of and solar collector absorber area in  $m^2$ . The parameter  $LCIE_{b,k}$  denotes the life cycle inventory of emissions of chemical  $b$  released during the construction phase per unit of capacity of equipment  $k$ . The values of  $LCIE_{b,k}$  should be obtained either from the literature or by performing an *ad hoc* LCA analysis on the construction of each single equipment.

The second term in eqn. (6) ( $LCI_b^{op}$ ) accounts for the emissions due to the extraction and combustion of natural gas, operation of the solar collectors

and generation of the cooling water and electricity consumed by the heat exchangers and pumps of the cycle, respectively:

$$\begin{aligned}
 LCI_b^{op} &= \sum_t \varphi T_{op} \left( Q_{k,t} LCI E_b^{heat(gfh)} + Q_{k',t} LCI E_b^{heat(col)} \right. \\
 &\quad \left. + m_{j,t} LCI E_b^{cw} + W_{k'',t} LCI E_b^{elec} \right) \\
 \forall b, j &= \text{cooling water}, k = GFH, k' = Col, k'' = Pump
 \end{aligned} \tag{8}$$

In this equation,  $T_{op}$  and  $\varphi$  are the annual operation hours of the cooling system and life span in years.  $LCIE_b^{heat(gfh)}$ ,  $LCIE_b^{heat(col)}$ ,  $LCIE_b^{cw}$  and  $LCIE_b^{elec}$  appearing in the same equation denote the life cycle inventory of emissions of chemical  $b$  contributing to global warming per unit of reference flow (*i.e.*, heat, amount of cooling water and electricity, respectively). These values, which can be retrieved from environmental databases [28, 29], depend on the particular features of the absorption cycle (*i.e.*, type of primary energy sources used in the heater, type of solar collectors, electricity mix of the country in which the cycle operates, etc.). Finally, the continuous variables  $m_{j=cooling\ water,t}$  and  $W_{k=Pump,t}$  denote the cooling water and electricity consumption, respectively, in period  $t$ . Note that the consumption of cooling water is obtained from the energy balance applied to the heat exchangers.  
*Impact assessment:* In this step, the life cycle inventory of emissions is translated into the corresponding contribution to global warming.

$$GWP = \sum_b LCI_b^{tot} df_b \tag{9}$$

Here, the parameter  $df_b$  is a damage factor that accounts for the global warming potential of chemical  $b$  compared to that of  $CO_2$ . These values are available in the *IPCC* report [30]. It should be noted that environmental databases such as Ecoinvent provide both the life cycle inventory of emissions as well as the associated environmental impacts per unit of reference flow. Hence, it might be possible to omit eqn.(9) in those cases in which the GWP values are directly available in the database.

*Interpretation:* In the context of the approach presented, the interpretation phase entails analyzing the Pareto solutions of the following multi-objective

environmental problem:

$$\begin{aligned}
 \text{(M)} \quad & \min_x U(x) = \{TC(x), GWP(x)\} \\
 \text{s.t.} \quad & h(x) = 0 \\
 & g(x) \leq 0 \\
 & x \in \mathfrak{R}
 \end{aligned} \tag{10}$$

In this formulation,  $x$  denotes state or design variables (*i.e.*, thermodynamic properties, flows, operating conditions, and sizes of equipment units). The equality constraints  $h(x) = 0$  represent thermodynamic property relations, mass and energy balances, cost, and LCA calculations. On the other hand, the inequality constraints  $g(x) \leq 0$  are added to model design specifications (*i.e.*, capacity limits, bounds on process variables, etc.). The objective function includes two terms:  $TC(x)$  is the total cost of the cooling system, and  $GWP(x)$  represents its environmental impact (*i.e.*, contribution to global warming). The solution to this problem is given by a set of efficient or Pareto optimal points representing trade-off designs [12].

#### 4. Solution method

To obtain the Pareto solutions of model (M), we apply the  $\epsilon$ -constraint method, which is based on solving a set of instances of an auxiliary model (MA) for different target values on the environmental performance (*i.e.*,  $GWP(x)$ ) as follows:

$$\begin{aligned}
 \text{(MA)} \quad & \min_x U(x) = TC(x) \\
 \text{s.t.} \quad & GWP(x) \leq \epsilon \\
 & \underline{\epsilon} \leq \epsilon \leq \bar{\epsilon} \\
 & h(x) = 0 \\
 & g(x) \leq 0 \\
 & x \in \mathfrak{R}
 \end{aligned} \tag{11}$$

Note that the lower and upper limits imposed on epsilon can be obtained by minimizing each scalar objective separately.

## 5. Case study

The capabilities of the proposed approach were illustrated through a case study that addresses the design of a solar assisted absorption cooling system with 100 kW cooling capacity. The process data for the absorption cycle are given in [14, 25]. We considered a water cooled ammonia/water absorption chiller with a generator temperature in the range of 95 to 120°C. Note that this temperature range cannot be reached by flat plate collectors with acceptable efficiencies [26] with acceptable efficiencies. For this reason in this work assumed to operate with evacuated tube collectors. More precisely, the cycle operates with a Sydney SK-6 from Microterm Energietechnik GmbH, which is a directly cooled evacuated tube collector with a cylindrical absorber and a CPC concentrator collector [8]. Global daily solar radiation of Barcelona (see Table 1) for an azimuth angle 0° and an inclination of 45° was considered [31].

*[Table 1 could be placed here]*

The entries of the life cycle inventory of GHG emissions associated with the construction and operation of the cooling system were defined as follows:

- *Heat exchangers:* The life cycle inventory of GHG emissions released during the construction of the heat exchangers was approximated by that associated with production of the equivalent mass of stainless steel. This amount of mass can be easily determined from the exchange area. The associated environmental information was taken from Ecoinvent [24].
- *Solar collectors:* The emissions due to the construction and operation of the evacuated tube collector were retrieved from Ecoinvent [24]. The operation emissions account for the maintenance of the solar collector and the generation of the electricity consumed by its pump.
- *Gas fired heater:* The emissions associated with the generation and combustion of natural gas in the fired heater were retrieved from Ecoin-

vent. This term accounts for the emissions given by the fuel generation, construction of the boiler, direct emissions, and electricity consumed during the boiler operation. For the calculations, we assumed an average net efficiency of 0.95 based on the lower heating value.

- *Pump*: The life cycle inventory of GHG emissions associated with the electricity consumed by the pump considering the electricity mix of Spain, was also retrieved from Ecoinvent [24]. The emissions during the construction of the pump and expansion valve were neglected.

## 6. Results and Discussions

### 6.1. Pareto set for the base case

The NLP model of the solar assisted cooling system was implemented in GAMS 23.0 [28] and solved with the NLP solver CONOPT [29] in a 2.29 GHz machine. The Pareto solutions were calculated following the method described before. The model contained 2634 constraints and 2116 variables. It took 22 seconds of CPU time to generate 21 Pareto solutions.

Fig. 3 depicts the Pareto set of alternatives, each of which represents a different integrated absorption cycle with a specific solar fraction. The y axis on the right hand side of the figure shows the solar fraction associated with each Pareto design (*i.e.*, amount of energy covered by solar energy divided by the total energy consumed by the cycle), whereas that on the left axis provides the total cost.

[*Figure 3 could be placed here*]

As can be seen, there is a clear trade off between the economic (total cost) and environmental (GWP) indicators. Particularly, one can reduce up to 82.3% the GWP potential at the expense of increasing the total cost by 115%. Further inspection of the Pareto points reveals that reductions in GWP with respect to the minimum cost design are achieved by reducing the primary

energy consumption rate of the cycle. This is accomplished by increasing the area of the heat exchangers of the cycle and also by replacing the primary energy source (natural gas) by solar energy. Note that reducing the natural gas consumption decreases the operating cost of the cooling system, but also increases the capital cost due to the installation of solar collectors. In practice, the latter effect dominates the former one, so an increase in the total cost is observed when the GWP is minimized.

As observed in the figure, the slope of the Pareto curve is smooth in the region close to the minimum cost design (point D), but becomes steeper as we move towards the minimum GWP solution (point A). This is because in order to fulfill more stringent environmental limitations (near to Pareto design A), the model is forced to increase the area of the solar collectors drastically in order to cover the energy requirements in months with low radiations. This causes a large increase in the slope of the curve, as observed in the figure.

In Fig. 3 we have also depicted the economic and environmental performance of a standard vapour compression chiller, considering only the impact during the operation phase. This chiller has a cooling capacity of 100 kW and a  $COP$  of 3. Data for the Spanish electricity grid retrieved from Ecoinvent [24] was considered in its environmental assessment. A simulation model of the chiller was implemented in EES [32] in order to perform the calculations. As observed, this system dominates part of the Pareto designs, as it shows better environmental and economic performance for a GWP above 2100  $ton CO_{2eq}$ . However, the vapour compression chiller have the limitation that it cannot reduce the GWP below that point. Hence, it can be concluded from these results that depending on the part of the Pareto frontier in which decision-makers are interested, it might be convenient to select a traditional vapour compression cycle instead of a solar assisted cooling system.

*[Figure 4 could be placed here]*

Fig. 4 depicts for some of the Pareto designs shown in Fig. 3, the solar fraction attained in each month of the year. Note that the model assumes that the cycle operates in the same way during all the years of the time horizon. As seen, in the minimum environmental impact design (design A), 98% of the heat demanded by the absorption chiller is covered by solar energy. On the other hand, in the Pareto designs B, C, and D the contribution of the solar energy decreases depending on the environmental limit imposed by the epsilon constraint method. Pareto design D is not visible in the figure because at the minimum total cost design the cooling system does not have any contribution of solar energy.

*[Figure 5 could be placed here]*

Fig. 5 shows the life cycle GWP associated with the operation of the cycle for some Pareto alternatives (*i.e.*, points A, B, C and D in Fig. 3) in each month of the year. As we can see in Fig. 5, the GWP is lower in May, June, July and August, due to the high global daily solar radiation (see Table 1). In these months, the natural gas consumption is reduced and the GHG emissions are decreased.

## 6.2. Taxes on GHG emissions

Ideally, decision-makers should analyze the Pareto set of alternatives given in Fig. 3, and finally choose the best one according to their preferences. Unfortunately, this is not done in practice. Instead, the total cost is usually minimized as single-objective and the unique solution obtained by doing so is implemented as far as it fulfills the environmental legislation. Hence, by setting taxes on GHG emissions, policy makers can guide decision-makers towards the adoption of more sustainable alternatives.

With this observation in mind, we conducted an analysis whose goal was to assess the impact of a given tax on  $CO_2$  emissions on the optimal absorption cycle configuration considering only its economic performance. More precisely, we aimed at determining how the areas of the heat exchangers of



the cycle and number of solar collectors changed as a function of the charges  $tax_{CO_2}$  on the  $CO_2$  emissions. This study was performed by solving the following single-objective optimization model that minimizes the total cost for different possible values of  $tax_{CO_2}$ :

$$\begin{aligned}
\text{(MT)} \quad & \min_x \quad U(x) = TC(x) + GWP(x)tax_{CO_2} \\
& \text{s.t.} \quad h(x) = 0 \\
& \quad \quad g(x) \leq 0 \\
& \quad \quad x \in \mathfrak{R}
\end{aligned} \tag{12}$$

Note that this is indeed equivalent to applying the weighted sum method (REF) to the multi-objective problem (M). In fact, each single run of model (MT) for a given tax value on the GHG emissions provides a different Pareto solution. Conversely, each point of the Pareto set “total cost” vs “GWP” has an associated tax rate, that is to say, a value of the tax rate that would make that Pareto point optimal if the total cost was minimized as a single objective without any restriction on the GHG emissions. It should be noted that since the problem is nonconvex, the weighted sum method is not guaranteed to provide all the solutions of the Pareto set. In fact, it can only provide the points that lie in the convex envelope of the Pareto set [33]. This implies that there might be points of the Pareto set that cannot be obtained by solving (MT) (*i.e.*, there is not any tax rate for which the Pareto point is the maximum of MT).

[*Table 2 could be placed here*]

The results obtained by applying the above commented procedure are given in Table 2. The table shows for each tax rate value, the total cost, GWP and solar fraction of the cycle that minimizes the cost as unique criterion. As observed, increasing the tax rate has the effect of leading to optimal designs with larger solar fractions and consequently less GHG emissions. This is an interesting result that shows how policy makers can influence on the GHG emissions in the energy sector by properly adjusting the tax rates. It

is worthwhile to mention that in the last Pareto optimal high jump in the total cost is observed. This could be explained that once the solar energy contribution reaches certain percentage further increase in the solar fraction alone does not lead to a reduction in environmental load but also it has to be accompanied by significant increase in the area of the absorption cycle. The increase in the area of the absorption cycle allows decreasing the higher temperature energy demand thus reducing the primary energy needs. However, it leads to a large increase of the total cost.

### 6.3. Influence of fuel cost

We recalculated next the Pareto set shown in Fig. 3 for different fuel prices in order to assess the impact of this parameter on the performance of the integrated system. Fig. 6 shows the new Pareto sets obtained for different fuel prices.

**[Figure 6 could be placed here]**

As expected, the Pareto set moves upwards and to the left when the fuel cost is increased. Particularly, the minimum total cost design shows a solar fraction of 8% for a fuel price of 0.0635 €/kWh, and of 77% when the fuel price is 0.0700 €/kWh. This is due to the fact that the increase in the fuel cost makes the integration of the cycle with solar collectors more profitable.

**[Table 3 could be placed here]**

Table 3 shows for each Pareto point in Fig. 6, the carbon dioxide tax rate ( $tax_{CO_2}$ ), the solar fraction ( $SF$ ) and the associated GWP for fuel prices of 0.0474 €/kWh, 0.0635 €/kWh and 0.07 €/kWh. Note that the tax rate given in the table is that for which the Pareto point would become optimal considering only the total cost as single objective.

As observed, by increasing the fuel cost, we get larger solar fractions and lower tax rates. This is an interesting observation that suggests that the tax

rate should be adapted to the cost data in order to achieve always a given reduction in GHG emissions rather than being fixed independently of the market trends.

Results in Table 3 indicate also that at a given fuel cost, it is possible to obtain Pareto designs with significant reductions in GWP by slightly increasing the tax rate on  $CO_2$  emissions. For instance, for a fuel cost of 0.0474 €/kWh and a tax rate of 77.8 €/ton  $CO_2$ , the optimal solar fraction is 0.06. However, by slightly increasing the value of  $tax_{CO_2}$  up to 4.4%, we obtain a solar fraction of 0.75 and a reduction of GWP of 62.8%. Moreover, Table 3 shows that when the fuel cost is increased to 0.07 €/kWh, the first four Pareto designs show a negative value of the charges on  $CO_2$  emissions. This is because in these cases the use of solar energy becomes profitable not only economically but also environmentally.

*[Figure 7 could be placed here]*

Fig. 7 depicts (1) the total life cycle GWP, the life cycle GWP associated with the manufacturing (2) and operation (3) of the cooling system, and (4) the  $CO_2$  emissions released during the cycle operation for the minimum total cost solution under different fuel prices. The emissions values were determined as follows: (4) includes the  $CO_2$  released in the combustion of natural gas in the fired heater; (3) accounts for the same emissions as in (4) plus those associated with the generation of the electricity and natural gas consumed by the cycle; (2) includes the life cycle GHG emissions associated with the construction of the cycle; and (1) is the summation of (2) and (3).

As observed, for high fuel cost values, the model tends to select the solar energy over the natural gas. Consequently, the GWP is reduced because the GHG emissions released during the operation of the cycle are decreased. This reduction in GWP is not significant for fuel cost values lower than 0.065 €/kWh. This is because below this point the economic savings in fuel expenditures are not compensated by the increase in capital cost due to

the purchase of solar collectors. Fig. 7 also shows how the GHG emissions released during the manufacturing phase can be neglected, since their contribution to the total GWP of the cycle is rather small. Furthermore, it can be observed how the GHG emissions released in the combustion of natural gas represent a large percentage of the total life cycle GHG emissions of the process.

It should be noted that the results obtained in the environmental analysis depend largely on the data used to calculate the life cycle inventory, which in our case were retrieved from the Ecoinvent database.

## 7. Conclusions

This paper has addressed the use of solar collectors coupled with absorption cooling cycles as a manner to reduce the GHG emissions in the cooling sector. The design of these systems has been formulated in mathematical terms as a multi-objective nonlinear programming (NLP) problem that seeks to minimize simultaneously the economic and environmental performance of the cooling application.

This work has extended our previously developed methodology [25] in the following ways: (i) it focuses on a different environmental performance measure (*i.e.*, global warming potential, GWP); (ii) it includes the option of using solar energy as a heat source to activate the cooling system; (iii) it assesses the impact that taxes on GHG emissions have on the optimal absorption cycle configuration considering only the economic performance; and (iv) it evaluates the impact of the fuel cost on the performance of the integrated system.

The results obtained show that with the current energy price and without considering governmental subsidies on solar technologies, the use of solar energy in cooling applications is not profitable.

The method presented in this paper is aimed at facilitating the task of policy makers when deciding on the tax rates to be fixed in order to promote more sustainable technological alternatives in the energy sector.

## 8. Nomenclature

### Abbreviations

<i>AB</i>	Absorber
<i>ABS</i>	Absorption cycle
<i>AC</i>	Air conditioning
<i>Col</i>	Solar collector
<i>Con</i>	Condenser
<i>D</i>	Desorber
<i>E</i>	Evaporator
<i>ETC</i>	Evacuated tube collector
<i>Exp</i>	Solution and subcooler expansion valve
<i>GFH</i>	Gas fired heater
<i>GHG</i>	Greenhouse gas emissions
<i>IPCC</i>	Intergovernmental Panel on Climate Change
<i>LCA</i>	Life cycle assessment
<i>NLP</i>	Nonlinear programming
<i>Pump</i>	Solution pump
<i>SC</i>	Subcooler
<i>SHX</i>	Solution heat exchanger

### Indices

<i>b</i>	Chemical emission
<i>i</i>	Component of a stream
<i>j</i>	Streams
<i>k</i>	Equipment unit of the absorption cycle
<i>t</i>	Time period

### Sets

<i>IN(k)</i>	Set of input streams to unit <i>k</i>
<i>OUT(k)</i>	Set of out put streams from unit <i>k</i>

## Parameters

$A_{col}$	Absorber area of solar collector model $i$ [ $m^2$ ]
$cost_{col}$	Specific cost of solar collector model $i$ [ $\frac{\text{€}}{m^2}$ ]
$cost_{elec}$	Specific cost of electricity [ $\frac{\text{€}}{kWh}$ ]
$cost_{ng}$	Specific cost of heat from natural gas [ $\frac{\text{€}}{kWh}$ ]
$c_0$	Optical efficiency value of solar collector model
$c_1$	Linear loss coefficient of solar collector model
$c_2$	Quadratic loss coefficient of solar collector model
$CEPCI_{1996}$	Chemical engineering cost index in year 1996
$CEPCI_{2008}$	Chemical engineering cost index in year 2008
$FC$	Fuel cost [ $\text{€}/kWh$ ]
$G_t$	Global daily solar radiation in period $t$ [ $\frac{W}{m^2}$ ]
$IAM(\Theta)$	Incident angle modifier [-]
$ir$	Interest rate [-]
$LCIE_b^{cw}$	Life cycle inventory entry associated with chemical $b$ per kg of cooling water used [ $\frac{kg}{unit}$ ]
$LCIE_b^{elec}$	Life cycle inventory entry associated with chemical $b$ per reference flow of electricity consumed [ $\frac{kg}{MJ}$ ]
$LCIE_b^{heat(col)}$	Life cycle inventory entry associated with chemical $b$ per kWh of heat delivered by the solar collector [ $\frac{kg}{kWh}$ ]
$LCIE_b^{heat(gh)}$	Life cycle inventory entry associated with chemical $b$ per MJ of heat delivered by the heater [ $\frac{kg}{MJ}$ ]
$LCIE_{b,k}$	Life cycle inventory entry associated with chemical $b$ per unit of capacity of equipment $k$ constructed [ $\frac{kg}{unit}$ ]
$T_t^{amb}$	Ambient temperature in period $t$ [ $^{\circ}C$ ]
$T_{op}$	Operational hours per year [ $\frac{h}{yr}$ ]
$U_k$	Overall heat transfer coefficient of unit $k$ [ $\frac{kW}{m^2K}$ ]
$\alpha_k$	Purchase cost exponent of unit $k$ [-]
$\beta_k$	Purchase cost coefficient [-]
$\epsilon$	Auxiliary parameter
$\underline{\epsilon}$	Lower bound on the auxiliary parameter $\epsilon$
$\bar{\epsilon}$	Upper bound on the auxiliary parameter $\epsilon$

$\eta^{gfh}$	Thermal efficiency of the gas fired heater [-]
$\eta^{mot}$	Compressor motor efficiency [-]
$\psi$	Capital cost coefficient [-]
$\theta$	Capital cost recovery factor [-]
$\Theta$	Incident angle
$\varphi$	Life span of the cooling system [ <i>years</i> ]
$df_b$	Global warming potential of chemical $b$ with respect to $CO_2$ [ $kg CO_{2eq}$ ]

### Variables

$A_k$	Area of heat exchanger $k$ [ $m^2$ ]
$CAP_k$	Capacity of equipment $k$
$CC_k$	Capital cost of equipment $k$ [€]
$COP$	Coefficient of performance of the absorption cycle [-]
$GWP$	Global warming potential [ $kg CO_{2eq}$ ]
$LCI_b^{man}$	Life cycle inventory of chemical $b$ associated with the manufacture of the cooling system [ $kg$ ]
$LCI_b^{op}$	Life cycle inventory entry of chemical $b$ associated with the operation of the cooling system [ $kg$ ]
$LCI_b^{tot}$	Total life cycle inventory entry of chemical $b$ [ $kg$ ]
$h_{j,t}$	Enthalpy of stream $j$ in period $t$ [ $\frac{kJ}{kg}$ ]
$m_{j,t}$	Mass flow rate of stream $j$ in period $t$ [ $\frac{kg}{s}$ ]
$n$	Number of collectors (relaxed integer variable)
$PEC_k$	Purchase cost of unit $k$ [€]
$P_{j,t}$	Pressure of stream $j$ in period $t$ [ $bar$ ]
$Q_{k,t}^{IN}$	Heat input to unit $k$ in period $t$ [ $kW$ ]
$Q_{k,t}^{OUT}$	Heat output from unit $k$ in period $t$ [ $kW$ ]
$RC_{cw}$	Running cost associated with cooling water consumption [€]
$RC_{gfh}$	Running cost of the gas fired heater [€]
$RC_{pump}$	Running cost of the pump [€]
$SF_t$	Solar fraction in period $t$ [-]
$tax_{CO_2}$	Tax on carbon dioxide emissions [€/ $ton CO_2$ ]

$TC$	Total cost [€]
$TCC$	Total capital cost [€]
$TOC$	Total operating cost [€]
$T_t^{av}$	Average temperature of collector inlet and exit temperatures in period $t$ [ $^{\circ}C$ ]
$T_{j,t}$	Temperature of stream $j$ in period $t$ [ $^{\circ}C$ or $K$ ]
$W_{k,t}$	Mechanical power of unit $k$ in period $t$ [ $kW$ ]
$x_{i,j,t}$	Mass fraction of component $i$ in stream $j$ in period $t$ [–]
$\Delta T_{k,t}^c$	Temperature difference in the cold end of unit $k$ in period $t$ [ $^{\circ}C$ or $K$ ]
$\Delta T_{k,t}^h$	Temperature difference in the hot end of unit $k$ in period $t$ [ $^{\circ}C$ or $K$ ]
$\Delta T_{k,t}^{lm}$	Logarithmic mean temperature difference of unit $k$ in period $t$ [ $^{\circ}C$ or $K$ ]
$\eta_t^{col}$	Solar collector efficiency in period $t$



## **Acknowledgements**

Berhane H. Gebreslassie would like to acknowledge his gratitude for the financial support received from the University Rovira i Virgili, the Spanish Ministry of Education and Science (DPI2008-04099 and CTQ2009-14420-C02) and the Spanish Ministry of External Affairs (A/016473/08, HS2007-0006 and A/023551/09). We would also like to thank the MSc. student Melanie Jiménez for helping to produce the numerical result for the case studies.

## References

- [1] Commission of the European Communities . Towards a european strategy for the security of energy supply. Tech. Rep.; 2001.
- [2] PRé-Consultants. SimaPro 7 LCA software. The Netherlands ([www.pre.nl/simapro/default.htm](http://www.pre.nl/simapro/default.htm)); 2008.
- [3] Casals XG. Solar absorption cooling in spain: Perspectives and outcomes from the simulation of recent instalations. *Renewable Energy* 2006;31:1371–89.
- [4] McMullan JT. Refrigeration and the environment – issues and strategies for the future. *International Journal of Refrigeration* 2002;25:89–99.
- [5] Jaruwongwittaya T, Chen G. A review: Renewable energy with absorption chillers in thailand. *Renewable and Sustainable Energy Reviews* 2010;14(5):1437 –44.
- [6] Rosiek S, Batlles F. Integration of the solar thermal energy in the construction: Analysis of the solar-assisted air-conditioning system installed in *CIESOL* building. *Renewable Energy* 2009;34(6):1423 –31.
- [7] Doukas H, Patlitzianas KD, Kagiannas AG, Psarras J. Renewable energy sources and rationale use of energy development in the countries of gcc: Myth or reality? *Renewable Energy* 2006;31(6):755 –70.
- [8] Henning HM. *Solar-Assisted Air-Conditioning in Buildings*. Springer Wien/New York; ISBN: 3-211 - 00647-8; 2004.
- [9] Azapagic A, Clift R. The application of life cycle assessment to process optimisation. *Computers and Chemical Engineering* 1999;10:1509–26.
- [10] Azapagic A, Clift R. Life cycle assessment and multiobjective optimisation. *Journal of Cleaner Production* 1999;7:135–43.

- [11] Guillén-Gosálbez G, Caballero JA, Esteller LJ. Application of life cycle assessment to the structural optimization of process flowsheets. *Industrial & Engineering Chemistry Research* 2008;47:777–89.
- [12] Hugo A, Ciumei C, Buxton A, Pistikopoulos EN. Environmental impact minimization through material substitution: a multi-objective optimization approach. *Green Chemistry* 2004;6:407–17.
- [13] Chavez-Islas LM, Heard CL. Design and analysis of an ammonia-water absorption refrigeration cycle by means of an equation-oriented method. *Industrial & Engineering Chemistry Research* 2009;48(4):1944–56.
- [14] Gebreslassie BH, Guillén-Gosálbez G, Jiménez L, Boer D. Economic performance optimization of an absorption cooling system under uncertainty. *Applied Thermal Engineering* 2009;29:3491–500.
- [15] Misra RD, Sahoo PK, Gupta A. Thermoeconomic evaluation and optimization of an aqua-ammonia vapour-absorption refrigeration system. *International Journal of Refrigeration* 2006;29:47–59.
- [16] Gebreslassie BH, Medrano M, Mendes F, Boer D. Optimum heat exchanger area estimation using coefficients of structural bonds: Application to an absorption chiller. *International Journal of Refrigeration* 2010;33:529–37.
- [17] Bernier E, Maréchal F, Samson R. Multi-objective design optimization of a natural gas-combined cycle with carbon dioxide capture in a life cycle perspective. *Energy* 2010;35:1121–8.
- [18] Molyneaux A, Leyland G, Favrat D. Environomic multi-objective optimisation of a district heating network considering centralized and decentralized heat pumps. *Energy* 2010;35:751 –8.
- [19] Li H, Maréchal F, Burer M, Favrat D. Multi-objective optimization of an advanced combined cycle power plant including  $CO_2$  separation options. *Energy* 2006;31:3117 –34.

- [20] Svensson E, Berntsson T. Economy and  $CO_2$  emissions trade-off: A systematic approach for optimizing investments in process integration measures under uncertainty. *Applied Thermal Engineering* 2010;30(1):23–9.
- [21] IRAM-ISO 14040. Environmental management-Life cycle assesment-Principles and frame work. 2006.
- [22] Azapagic A. Life cycle assessment and its application to process selection, design and optimisation. *Chemical Engineering Journal* 1999;73:1–21.
- [23] Guillén-Gosálbez G, Grossmann IE. A global optimization strategy for the environmentally conscious design of chemical supply chains under uncertainty in the damage assessment model. *Computers & Chemical Engineering* 2010;34(1):42–58.
- [24] The ecoinvent Center. A competence centre of *ETH, PSI, EMA&ART*, <http://www.ecoinvent.ch/>. ecoinvent data v21.
- [25] Gebreslassie BH, Guillén-Gosálbez G, Jiménez L, Boer D. Design of environmentally conscious absorption cooling systems via multi-objective optimization and life cycle assesment. *Applied Energy* 2009;86:1712–22.
- [26] Kalogirou SA. Solar thermal collectors and applications. *Progress in Energy and Combustion Science* 2004;30(3):231 –95.
- [27] Gian-Kasper P, Stocker T, Midgley P, Tignor M. *IPCC* Expert Meeting on the Science of Alternative Metrics. 2009.
- [28] Brooke A, Kendrik D, Meeraus A, Raman R, Rosenthal RE. *GAMS - A User's Guide*. GAMS Development Corporation, Washington; 1998.
- [29] Drud A. *CONOPT* Solver Manual. ARKI Consulting and Development, Bagsvaerd, Denmark; 1996.

- [30] Solomon S, Qin D, Manning M, Chen Z, Marquis M, Averyt K, Tignor M, Miller HL. Contribution of working group I to the fourth assessment report of the intergovernmental panel on climate change. Tech. Rep. Cambridge University Press, Cambridge, United Kingdom and New York, NY, USA; 2007.
- [31] Generalitat de Catalunya, Departament d'Indústria, Comerç i Turisme. ATLAS DE RADIACIÓ SOLAR A CATALUNYA. *http : //www20.gencat.cat/docs/icaen*; 2000.
- [32] F-Chart Software. Engineering equation solver, (*EES*). [www.fchart.com](http://www.fchart.com).
- [33] Bérubé JF, Gendreau M, Potvin JY. An exact  $\epsilon$ -constraint method for bi-objective combinatorial optimization problems: Application to the traveling salesman problem with profits. *European Journal of Operational Research* 2009;194(1):39 – 50.
- [34] Pátek J, Klomfar J. Simple functions for fast calculations of selected thermodynamic properties of the ammonia-water system. *International Journal of Refrigeration* 1995;18:228–34.
- [35] Edgar TF, Himmelblau DM, Lasdon LS. Optimization of chemical processes. McGraw-Hill; 2001.
- [36] Bejan A, Tsatsaronis G, Moran M. Thermal Design & Optimization. John Wiley & Sons Inc.; 1996.
- [37] Turton R, Bailie RC, Whiting WB, Shaeiwitz JA. Analysis, Synthesis, and Design of Chemical Processes. Prentice Hall PTR, New Jersey; 2003.
- [38] Chemical Engineering. Chemical engineering plant cost index (*CEPCI*). Tech. Rep., Chemical engineering. [www.CHE.com](http://www.CHE.com); 2009.

## List of Figures

1	Environmental analysis of the electricity and thermal energy driven chillers. . . . .	32
2	Solar assisted absorption chiller. . . . .	33
3	Pareto optimal designs of the base case. . . . .	34
4	Solar fraction in each month for the selected Pareto optimal designs. . . . .	35
5	GWP during the operation of the cooling system for the selected Pareto optimal designs. . . . .	36
6	Pareto optimal designs for different fuel prices. . . . .	37
7	The minimum cost solutions GWP at different fuel costs of the Pareto sets given in Fig. 6. In the figure, (1) refers to the total life cycle GWP; (2) to the life cycle GWP associated with the manufacturing of the cycle; (3) to the life cycle emissions during the operation of the cooling system; and (4) to the $CO_2$ emissions in the gas fired heater. . . . .	38

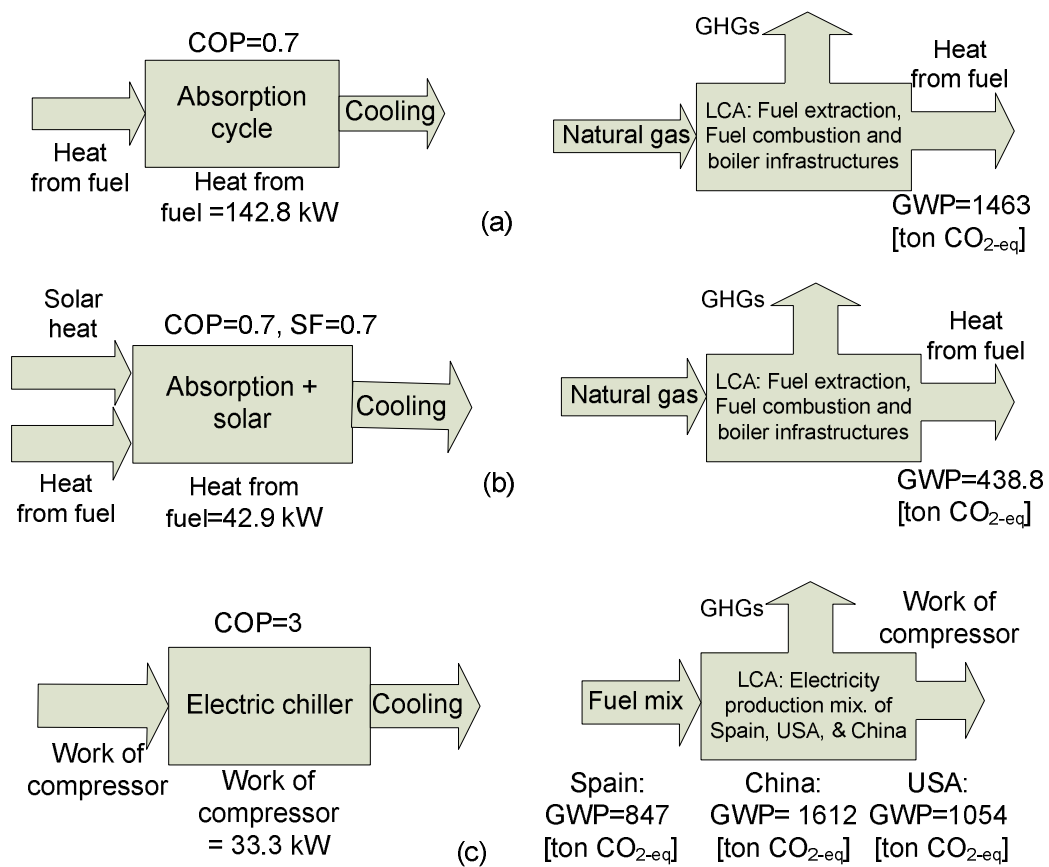


Figure 1: Environmental analysis of the electricity and thermal energy driven chillers.

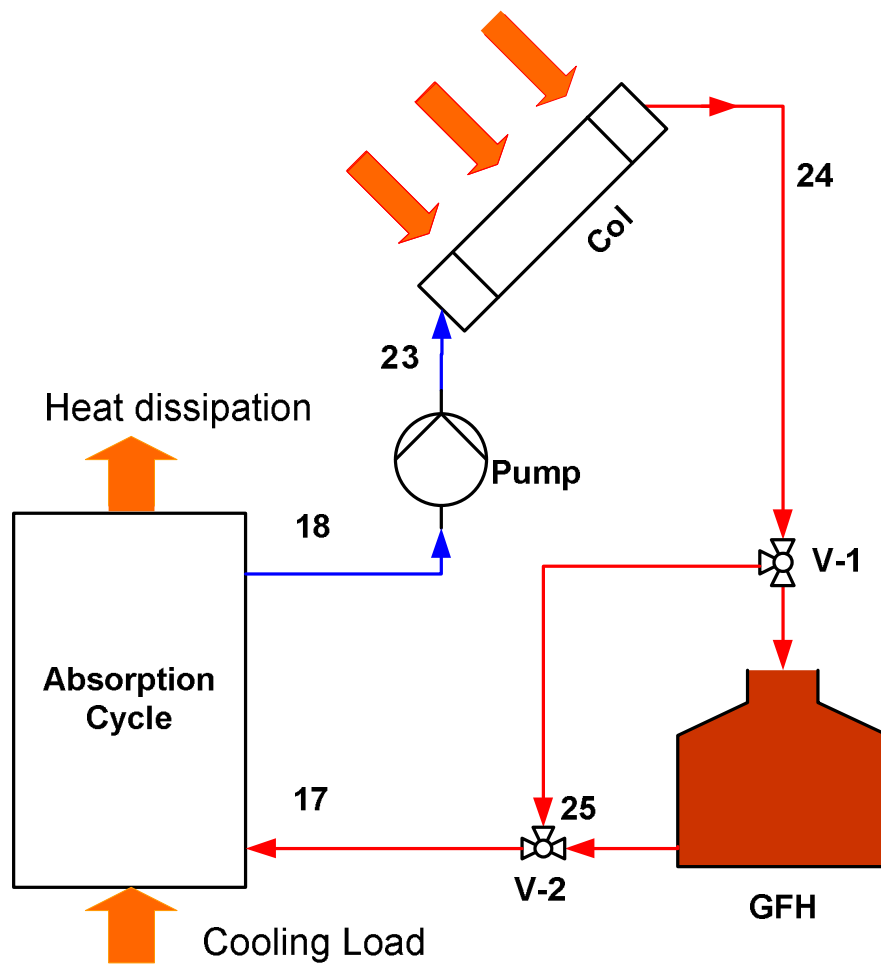


Figure 2: Solar assisted absorption chiller.



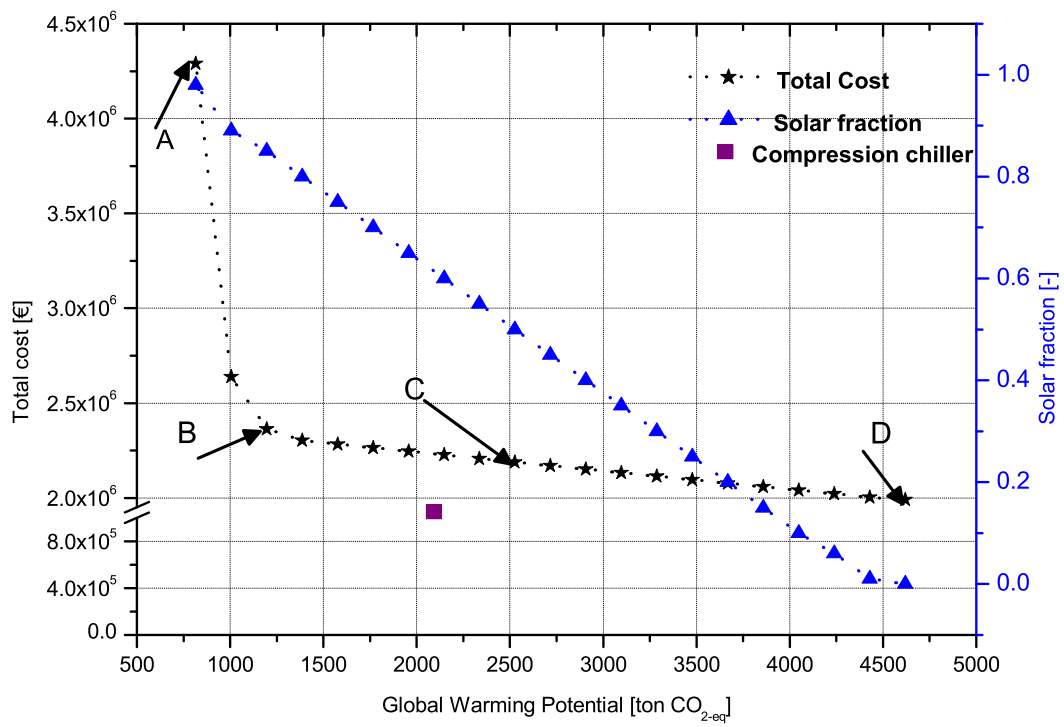


Figure 3: Pareto optimal designs of the base case.

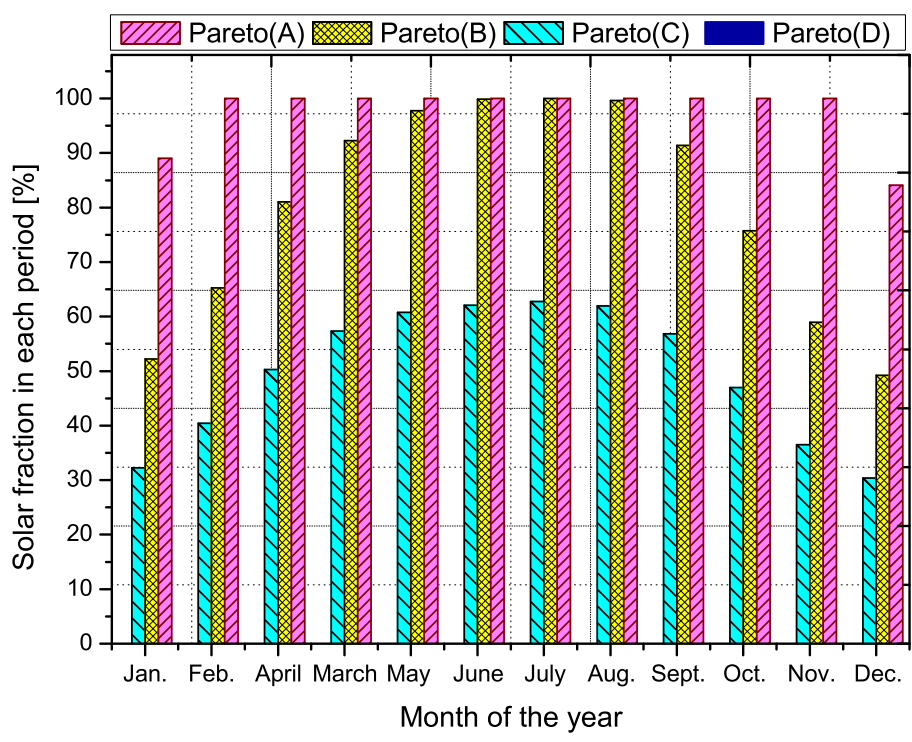


Figure 4: Solar fraction in each month for the selected Pareto optimal designs.

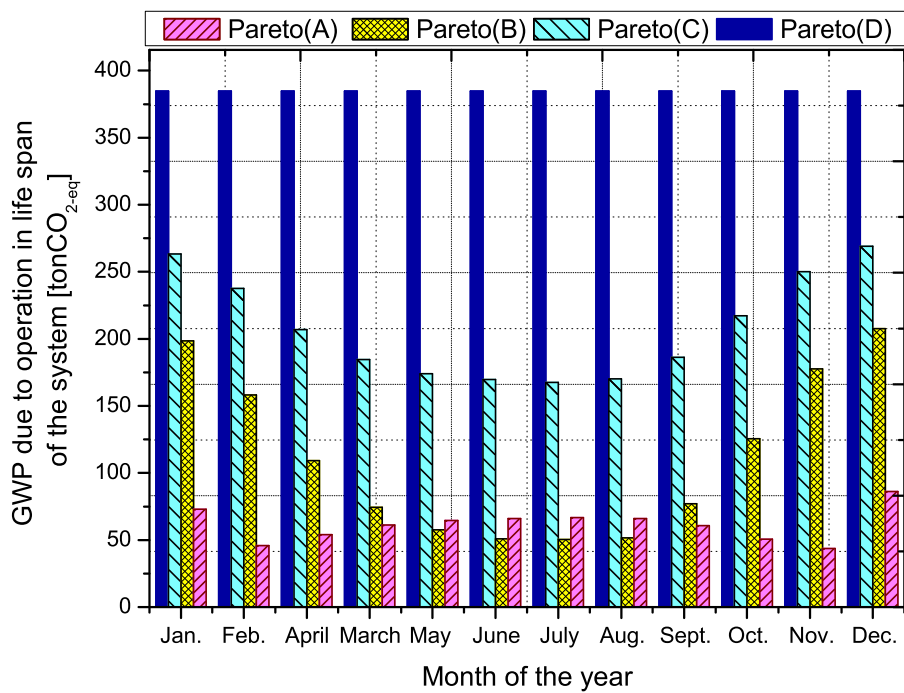


Figure 5: GWP during the operation of the cooling system for the selected Pareto optimal designs.

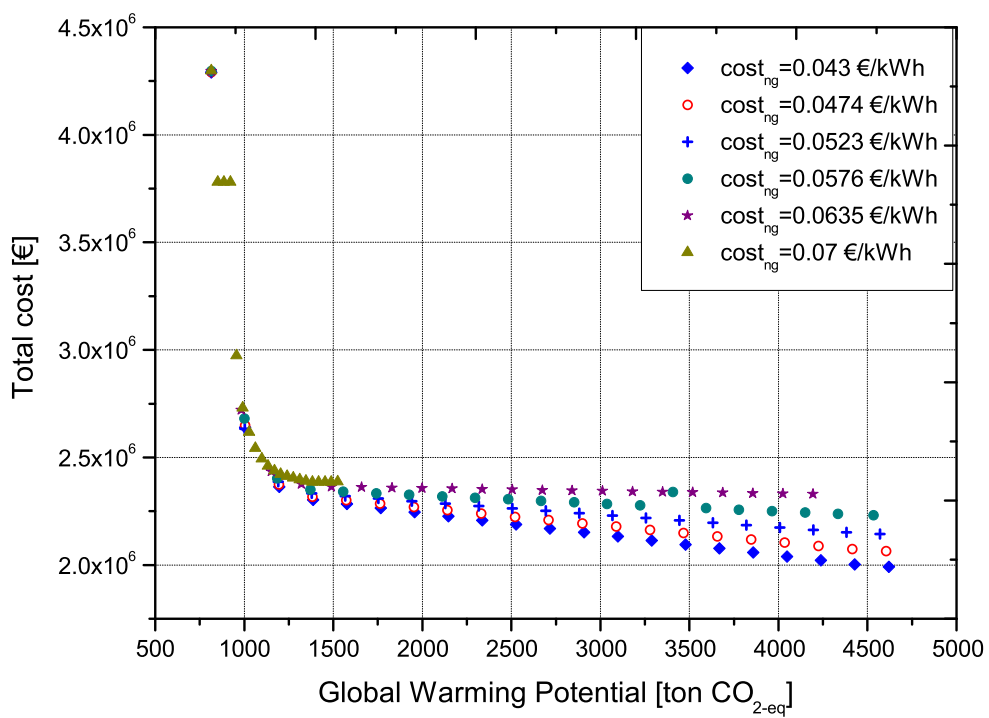


Figure 6: Pareto optimal designs for different fuel prices.

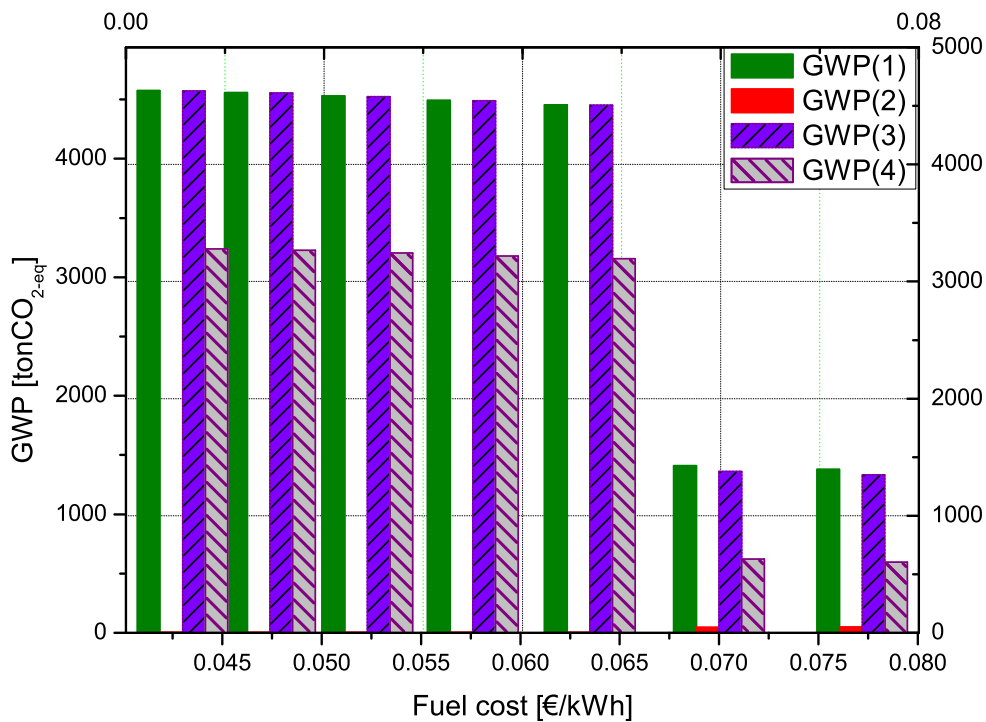


Figure 7: The minimum cost solutions GWP at different fuel costs of the Pareto sets given in Fig. 6. In the figure, (1) refers to the total life cycle GWP; (2) to the life cycle GWP associated with the manufacturing of the cycle; (3) to the life cycle emissions during the operation of the cooling system; and (4) to the  $CO_2$  emissions in the gas fired heater.

## List of Tables

1	Barcelona daily global solar radiation and ambient temperature for $45^0$ inclination. . . . .	40
2	The Pareto optimal design $tax_{CO_2}$ and solar fraction of Fig. 3. . . . .	41
3	GWP, Solar fraction and $tax_{CO_2}$ for some of the fuel costs of the Pareto optimal designs shown in Fig. 6. . . . .	42
B.4	Economic Parameters . . . . .	47

Table 1: Barcelona daily global solar radiation and ambient temperature for  $45^{\circ}$  inclination.

Period	$G_t$ [ $W/m^2$ ]	$T_t^{amb}$ [ $^{\circ}C$ ]
January	297.0	8.2
February	350.7	9.4
March	415.3	11.1
April	460.4	13.1
May	478.5	17.0
June	482.4	20.9
July	483.8	23.5
August	477.5	24.1
September	445.8	21.6
October	385.0	17.3
November	320.6	12.1
December	282.2	9.9

Table 2: The Pareto optimal design  $tax_{CO_2}$  and solar fraction of Fig. 3.

TC [€]	GWP [ton CO <sub>2</sub> -eq]	$tax_{CO_2}$ [ $\frac{€}{ton CO_2}$ ]	SF [-]
1992007	4620	0.00	0.00
2260393	4429	58.10	0.01
2429149	4239	96.20	0.06
2430839	4049	96.60	0.10
2432453	3859	97.00	0.15
2434353	3669	97.50	0.20
2435437	3478	97.80	0.25
2436125	3288	98.00	0.30
2437741	3098	98.50	0.35
2438631	2908	98.80	0.40
2439192	2717	99.00	0.45
2439714	2527	99.20	0.50
2440204	2337	99.40	0.55
2440423	2147	99.50	0.60
2440626	1957	99.60	0.65
2435402	1766	96.64	0.70
2440797	1576	99.70	0.75
2448339	1386	104.50	0.80
2742809	1196	317.00	0.85
4098633	1005	1451.00	0.89
11365723	815	8679.00	0.98



Table 3: GWP, Solar fraction and  $tax_{CO_2}$  for some of the fuel costs of the Pareto optimal designs shown in Fig. 6.

GWP	fuel cost = 0.0474 $\frac{\text{€}}{\text{kWh}}$		fuel cost = 0.0635 $\frac{\text{€}}{\text{kWh}}$		fuel cost = 0.07 $\frac{\text{€}}{\text{kWh}}$			
	$tax_{CO_2}$ [ $\frac{\text{€}}{\text{ton} \cdot CO_2}$ ]	SF [-]	GWP	$tax_{CO_2}$ [ $\frac{\text{€}}{\text{ton} \cdot CO_2}$ ]	SF [-]	GWP	$tax_{CO_2}$ [ $\frac{\text{€}}{\text{ton} \cdot CO_2}$ ]	SF [-]
4604	0.0	0.00	4194	0.0	0.08	1524	-18.4	0.77
4414	48.7	0.01	4025	10.2	0.11	1489	-18.3	0.78
4225	77.8	0.06	3856	11.0	0.16	1453	-14.1	0.79
4035	78.5	0.11	3687	11.3	0.20	1418	-11.2	0.80
3846	78.8	0.16	3518	11.6	0.24	1382	20.9	0.80
3657	79.0	0.21	3349	11.9	0.29	1347	109.0	0.81
3467	79.5	0.25	3180	12.2	0.33	1311	175.5	0.82
3278	79.8	0.30	3011	12.4	0.37	1276	221.8	0.83
3088	80.0	0.35	2842	12.6	0.42	1241	225.0	0.84
2899	80.3	0.40	2674	12.8	0.46	1205	271.5	0.85
2709	80.6	0.45	2505	13.0	0.51	1170	477.0	0.86
2520	80.7	0.50	2336	13.1	0.55	1134	636.0	0.86
2331	80.8	0.55	2167	13.2	0.60	1099	935.0	0.87
2141	81.0	0.60	1998	13.2	0.64	1063	1398.0	0.88
1952	81.0	0.65	1829	13.3	0.69	1028	2082.5	0.89
1762	81.1	0.70	1660	13.3	0.73	992	3180.0	0.89
1573	81.2	0.75	1491	13.3	0.78	957	6861.0	0.90
1383	86.5	0.80	1322	69.5	0.82	922	7597.1	0.91
1194	304.0	0.85	1153	356.5	0.86	886	7597.1	0.91
1005	1460.0	0.89	984	1694.0	0.90	851	7597.1	0.91
815	8671.0	0.98	815	9325.0	0.98	815	14608.0	0.98

# Appendices

## Appendix A. Energy and material balance applied to each unit of the cooling system

The model of the integrated absorption cycle is based on mass and energy conservation laws. It includes also equations for assessing the economic and environmental performance of the cooling system. We provide next the main constraints of the model. Further details can be found in [14, 25].

- Mass balance: The total mass of component  $i$  that enters unit  $k$  in period  $t$  is equal to the total mass of the same component  $i$  that leaves the unit.

$$\sum_{j \in IN(k)} m_{j,t} x_{i,j,t} - \sum_{j \in OUT(k)} m_{j,t} x_{i,j,t} = 0 \quad \forall k, i, t \quad (\text{A.1})$$

In this equation,  $m_{j,t}$  is the mass flow rate of stream  $j$  in time period  $t$ ,  $x_{i,j,t}$  is the composition of component  $i$  in stream  $j$  and period  $t$ , and  $IN(k)$  and  $OUT(k)$  are the set of input and output streams associated with unit  $k$ .

- Energy balance: The difference in heat content between the inlet and outlet streams of a unit  $k$  plus the difference in heat supplied ( $Q_{k,t}^{IN}$ ) and removed ( $Q_{k,t}^{OUT}$ ) minus the work done ( $W_{k,t}$ ) must equal zero in each period  $t$ . Furthermore, the input and output heat terms are zero in some units of the cycle.

$$\sum_{j \in IN(k)} m_{j,t} h_{j,t} - \sum_{j \in OUT(k)} m_{j,t} h_{j,t} + Q_{k,t}^{IN} - Q_{k,t}^{OUT} - W_{k,t} = 0 \quad \forall k, t \quad (\text{A.2})$$

$$Q_{k,t}^{IN} = 0 \quad \text{if} \quad k = \left\{ \begin{array}{l} \text{Absorber (AB)} \\ \text{Condenser (Con)} \\ \text{Subcooler (SC)} \\ \text{Solution heat exchanger (SHX)} \\ \text{Pump (Pump)} \\ \text{Expansion valves (Exp)} \end{array} \right\} \quad (\text{A.3})$$

$$Q_{k,t}^{OUT} = 0 \quad \text{if} \quad k = \left\{ \begin{array}{l} \text{Evaporator (E)} \\ \text{Desorber (D)} \\ \text{Subcooler (SC)} \\ \text{Solution heat exchanger (SHX)} \\ \text{Pump (Pump)} \\ \text{Expansion valves (Exp)} \\ \text{Solar collectors (Col)} \\ \text{Gas fired heater, (GFH)} \end{array} \right\} \quad (\text{A.4})$$

$$W_{k,t} = 0 \quad \forall k \neq \text{Pump} \quad (\text{A.5})$$

In eqn. (A.2),  $h_{j,t}$  denotes the specific enthalpy of stream  $j$  in period  $t$ .

- The thermodynamic properties of the ammonia-water working pair are determined with the correlations of Patek and Klomfa [34]

$$h_{j,t} = f(T_{j,t}, P_{j,t}, x_{i,j,t}) \quad \forall t \quad (\text{A.6})$$

where,  $T_{j,t}$  and  $P_{j,t}$  are the temperature and pressure of stream  $j$  in period  $t$ , and  $x_{i,j,t}$  is the mass fraction of component  $i$  in stream  $j$  in period  $t$

- The heat exchangers are modeled based on the logarithmic mean temperature difference, as shown in eqn. (A.7).

$$Q_{k,t} = U_k A_k \Delta T_{k,t}^{lm} \quad k = AB, Con, D, E, SC, SHX, \quad \forall t \quad (\text{A.7})$$

Here,  $Q_{k,t}$  is the heat transfer in heat exchanger  $k$  in period  $t$ ;  $U_k$  is the overall heat transfer co-efficient;  $A_k$  is the heat transfer area of the heat exchanger  $k$ ; and  $\Delta T_{k,t}^{lm}$  is the logarithmic mean temperature difference.

- In order to improve the numerical performance of the model, the logarithmic mean temperature difference, which is a function of the hot

and cold end temperature differences ( $\Delta T_{k,t}^h$  and  $\Delta T_{k,t}^c$ , respectively), is calculated via the Chen's approximation [35], as shown in eqn. (A.8).

$$\Delta T_{k,t}^{lm} \cong \left[ \Delta T_{k,t}^h \Delta T_{k,t}^c \frac{\Delta T_{k,t}^h + \Delta T_{k,t}^c}{2} \right]^{\frac{1}{3}} \quad k = AB, Con, D, E, SC, SHX, \forall t \quad (\text{A.8})$$

- The total useful heat absorbed by the collector ( $Q_{k=Col,t}$ ) and the heat generated by the gas fired heater ( $Q_{k=GFH,t}$ ) in period  $t$  are determined using the following equations:

$$Q_{k,t} = m_{23,t} C_p (T_{24,t} - T_{23,t}) \quad k = Col, \forall t \quad (\text{A.9})$$

$$Q_{k,t} = m_{24,t} C_p (T_{25,t} - T_{24,t}) \quad k = GFH, \forall t \quad (\text{A.10})$$

in which the numbers refer to those in Fig. 2.

## Appendix B. Equations for calculating the capital and operation costs of the cooling system

- The capital cost of the cooling system includes the cost of the heat exchangers, solar collectors, gas fired heater, pump, and expansions valves, which are denoted by the continuous variable  $CC_k$ .

$$TCC = \varphi \theta \left( \sum_k CC_k \right) \quad (\text{B.1})$$

Here,  $\varphi$  is the life span of the cooling system and  $\theta$  is the capital recovery factor, which is determined from eqn. (B.2),

$$\theta = \frac{ir (ir + 1)^\varphi}{(ir + 1)^\varphi - 1} \quad (\text{B.2})$$

where  $ir$  is the annual interest rate. On the other hand, The capital cost of unit  $k$  is estimated from the purchase cost of the unit ( $PEC_k$ )

given by eqn. (B.5) and the cost parameter  $\psi$ , which has been taken from Bejan et al. [36].

$$CC_k = \psi PEC_k \quad \forall k \neq Col, \forall t \quad (\text{B.3})$$

The purchase cost of unit  $k$  in year 1996 ( $PEC_k^{1996}$ ) is estimated following Turton et al. [37].

$$PEC_k^{1996} = \beta_k (CAP_k)^{\alpha_k} \quad \forall k \neq Col \quad (\text{B.4})$$

Where  $CAP_k$  is the capacity measure of unit  $k$ .  $\alpha_k$  and  $\beta_k$  are the cost parameters, which are given in Table B.4, that have been obtained from Turton et al. [37]. The purchase equipment cost is updated from year 1996 to year 2008 using the Chemical Engineering plant cost index [38] as follows:

$$PEC_k = PEC_k^{1996} \frac{CEPCI_{1996}}{CEPCI_{2008}} \quad \forall k \quad (\text{B.5})$$

Here, the parameters  $CEPCI_{1996}$  and  $CEPCI_{2008}$  refer to the Chemical Engineering plant cost index in years 1996 and 2008, respectively.

The capital cost of the solar collector, which is given by eqn. (B.6), is a function of the number of collectors ( $n$ ), absorber area ( $A_{col}$ ) and collector cost per  $m^2$  of absorber area [8].

$$CC_k = nA_{col}cost_{col} \quad k = Col \quad (\text{B.6})$$

- The operating cost ( $TOC$ ) of the cooling system accounts for the running cost of the gas fired heater ( $RC_{gfh}$ ), the running cost of the pump ( $RC_{pump}$ ), and the cooling water cost ( $RC_{cw}$ ):

$$TOC = RC_{gfh} + RC_{pump} + RC_{cw} \quad (\text{B.7})$$

$$RC_{gfh} = \frac{cost_{ng}\varphi T_{op}}{12\eta^{gfh}} \left( \sum_t Q_{k,t} \right) \quad k = GFH \quad (\text{B.8})$$

$$RC_{pump} = \frac{cost_{elec}\varphi T_{op}}{12} \left( \sum_t W_{k,t} \right) \quad k = Pump \quad (B.9)$$

$$RC_{cw} = cost_{cw}\varphi T_{op} \left( \sum_t m_{j,t} \right) \quad j = cooling\ water \quad (B.10)$$

Where  $cost_{ng}$ ,  $cost_{elec}$  and  $cost_{cw}$  are the prices of the natural gas, electricity and cooling water, respectively.  $T_{op}$  and  $\eta^{gfh}$  denote the annual operating hours, and gas fired heater efficiency, respectively.

Table B.4: Economic Parameters

Unit	$\beta_k$	$\alpha_k$	Range
Heat exchanger	6880	0.430	5 – 1500m <sup>2</sup>
Gas fired heater	1633	0.584	100 – 10000kW
Pump	1942	1.110	1 – 100kW